

18.338 Project Report

Author: Rosen Yu (rosenyu@mit.edu)

October 29th, 2025

Code for all experiments: https://github.com/rosenyu304/18338_Project

Website app for Sturm histogramming and β -estimator: <https://huggingface.co/spaces/rosenyu/18338RMTProject>

1 Visualizing the β -Hermite Random Matrix Ensemble

1.1 Motivation

The β -Hermite ensemble is critical in random matrix theory as it generalizes the classical Gaussian ensembles ($\beta=1,2,4$ are GOE/GUE/GSE). For many computational tasks one wishes to visualize two fundamental spectral statistics: the eigenvalue density (semicircle law in the large- n limit) and the nearest-neighbor spacing distribution, parameterized by a single index β . Chan (2007) developed two tools that make this possible at scale:

- A **β -estimator** based on fitting the empirical spacings (Chan's public **Beta Estimator** (MIT, 2006)).
- A **Sturm-sequence-based histogramming algorithm** enabling eigenvalue histograms in $O(mn)$ time rather than the usual $O(n^2)$.

The original tools were written in Perl and C. My contribution in this project was to re-implement both methods in Julia and Python, verify their correctness using the mathematical formulas in the papers, and integrate them into an interactive Gradio web application hosted on Hugging Face. The resulting interface allows users to explore β -Hermite matrices, visualize eigenvalue distributions, and estimate β from empirical data in real time.

1.2 Sturm Sequence Histogramming for β -Hermite ensemble

The naive workflow for visualizing eigenvalue distributions is: (1) generate a β -Hermite tridiagonal matrix $H_\beta \in \mathbb{R}^{n \times n}$,

$$H_{\beta,n} \sim \frac{1}{\sqrt{2}} \begin{pmatrix} N(0, 2) & \chi_{(n-1)\beta} & & \\ \chi_{(n-1)\beta} & N(0, 2) & \chi_{(n-2)\beta} & \\ & \ddots & \ddots & \ddots \\ & & \chi_{2\beta} & N(0, 2) & \chi_\beta \\ & & & \chi_\beta & N(0, 2) \end{pmatrix}$$

(2) compute all eigenvalues using a standard routine which typically requires cost of $O(n^2)$, and (3) place them into histogram bins ($O(n + m)$). For large n , the dominant cost is the eigenvalue computation, which is fundamentally quadratic runtime $O(n^2)$.

The Sturm sequence algorithm replaces eigenvalue computation entirely. As shown in Albrecht et al. (2009), one may compute the number of eigenvalues of A in any interval (k_{i-1}, k_i) using only the recurrence relation for the Sturm ratio sequence and counts of sign changes. This yields an $O(mn)$ algorithm, dramatically improving performance since typically $m \ll n$.

1.2.1 Mathematical Background

This section is based on Chan (2007) and Albrecht et al. (2009). Given a symmetric tridiagonal matrix

$$A = \begin{bmatrix} a_1 & b_1 & & & \\ b_1 & a_2 & b_2 & & \\ & \ddots & \ddots & \ddots & \\ & & b_{n-1} & a_n & \end{bmatrix},$$

the Sturm sequence (d_0, d_1, \dots, d_n) is defined by determinants of trailing principal minors. It satisfies the recurrence:

$$d_0 = 1, \quad d_1 = a_1, \quad d_i = a_i d_{i-1} - b_{i-1}^2 d_{i-2}.$$

or equivalently, defining the Sturm ratio sequence

$$r_i = \frac{d_i}{d_{i-1}},$$

one obtains the simple recurrence:

$$r_1 = a_1, \quad r_i = a_i - \frac{b_{i-1}^2}{r_{i-1}}, \quad i \geq 2.$$

Why Sturm Sequences Count Eigenvalues The connection between Sturm sequences and eigenvalue counting relies on a classical result from the theory of symmetric matrices. For a symmetric tridiagonal matrix A , the eigenvalues of consecutive principal submatrices satisfy an interlacing property: if $\lambda_1(A_k) \leq \lambda_2(A_k) \leq \dots \leq \lambda_k(A_k)$ denote the eigenvalues of the $k \times k$ trailing principal submatrix, then

$$\lambda_i(A_k) \leq \lambda_i(A_{k+1}) \leq \lambda_{i+1}(A_k).$$

This interlacing property implies that when we evaluate the sequence of determinants d_0, d_1, \dots, d_n for $A - \lambda I$, a sign change from d_{k-1} to d_k occurs precisely when λ lies between two consecutive eigenvalues of A_k . Consequently, the number of sign changes in the Sturm sequence (d_0, d_1, \dots, d_n) equals the number of eigenvalues of A that are less than λ (Wilkinson (1988) and Trefethen and Bau (2022)).

Preservation of Sign Information via Ratios. Since we are only interested in counting sign changes rather than computing the determinants themselves, the Sturm ratio sequence $r_i = d_i/d_{i-1}$ provides an equivalent but numerically superior representation. A sign change from d_{i-1} to d_i occurs if and only if $r_i < 0$, thus

$$\#\{\text{negative eigenvalues of } A\} = \#\{i : r_i < 0\}.$$

The computational advantage of ratios is twofold: first, the recurrence relation

$$r_i = a_i - \frac{b_{i-1}^2}{r_{i-1}}$$

requires only $O(1)$ operations per term, compared to $O(i^2)$ for computing determinants via expansion of minors; second, ratios avoid the numerical overflow and underflow issues that plague direct determinant computation for large matrices.

From Eigenvalue Counts to Histograms The histogram algorithm exploits the following observation: to count the number of eigenvalues in an interval $(k_{i-1}, k_i]$, we compute

$$H_i = \Lambda(A - k_i I) - \Lambda(A - k_{i-1} I),$$

where $\Lambda(M)$ denotes the number of negative eigenvalues of matrix M . Since $\Lambda(A - k_j I)$ equals the number of eigenvalues of A less than k_j , the difference H_i gives precisely the count of eigenvalues falling within the i -th bin.

For each bin edge k_j , we construct the Sturm ratio sequence for $A - k_j I$ and count the number of negative ratios, yielding $\Lambda_j = \Lambda(A - k_j I)$ in $O(n)$ time. With m bin edges, this step requires $O(mn)$ total operations. The histogram values are then obtained via the simple differences

$$H_1 = \Lambda_1, \quad H_i = \Lambda_i - \Lambda_{i-1} \text{ for } 2 \leq i \leq m-1, \quad H_m = n - \Lambda_{m-1},$$

which can be computed in $O(m)$ time. The total complexity is thus $O(mn)$, compared to $O(n^2)$ for the naive approach of computing all eigenvalues via standard packages.

Algorithm 1 Sturm-Sequence Histogramming of a β -Hermite Matrix

Require: matrix dimension n , histogram bin edges $k_0 < \dots < k_m$,

β -Hermite diagonal a_i and off-diagonal b_i entries.

```
1: for each bin edge  $k_j$  do
2:   Initialize  $r_1 = a_1 - k_j$ ;
3:   count =  $1\{r_1 < 0\}$ ;
4:   for  $i = 2$  to  $n$  do
5:      $r_i = (a_i - k_j) - \frac{b_{i-1}^2}{r_{i-1}}$ ;
6:     count +=  $1\{r_i < 0\}$ ;
7:   end for
8:   Store  $\Lambda_j = \text{count}$ 
9: end for
10: Compute histogram bins
11:    $H_1 = \Lambda_1$ ,
12:    $H_i = \Lambda_i - \Lambda_{i-1}$ ,
13:    $H_m = n - \Lambda_{m-1}$ .
14: return  $H$ 
```

1.2.2 Numerical experimentation of Sturm sequence histogramming and Results

This study replicated the numerical experiment described in Albrecht et al. (2009) and confirmed the stated asymptotic behavior of both algorithms. Our naive eigenvalue-based histogramming exhibits the expected $O(n^2)$ growth, while the Sturm-sequence method grows linearly in both n and the number of bins m , matching the theoretical $O(mn)$ complexity. The experimentally measured runtimes, as demonstrated in Figure 1 and 2 below, reproduce the results in Albrecht et al. (2009), demonstrating that the bin-count has a negligible effect on the naive method and a bilinear effect on the Sturm method. Finally, the Sturm-based histogram in Figure 3 for the $\beta = 2$ Hermite ensemble closely matches the Wigner semicircle law, confirming the correctness of the implementation.

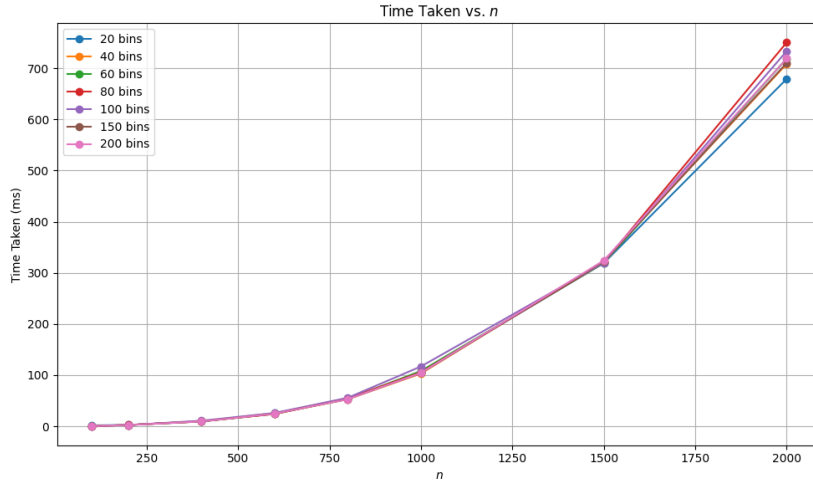


Figure 1: Naive histogramming time grows quadratically in n , consistent with the $O(n^2)$ eigenvalue computation cost. Here we plot the mean over 100 trials.

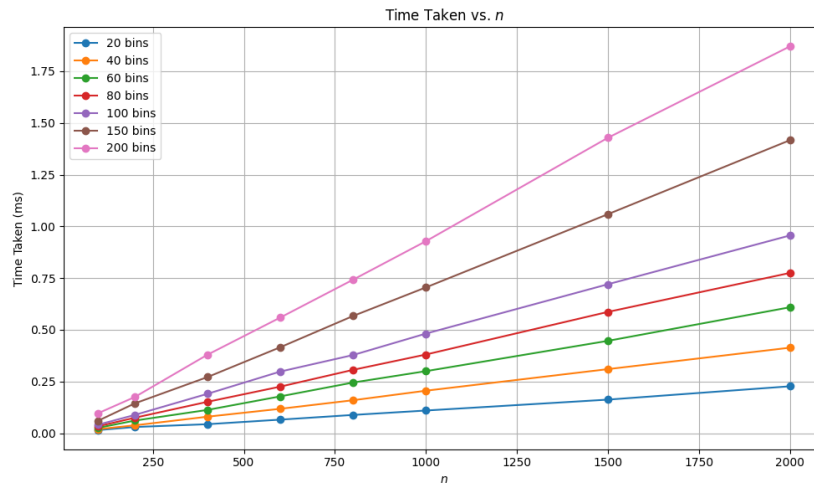


Figure 2: Sturm-sequence histogramming shows linear dependence on n and m , matching the predicted $O(mn)$ complexity. Here we plot the mean over 100 trials.

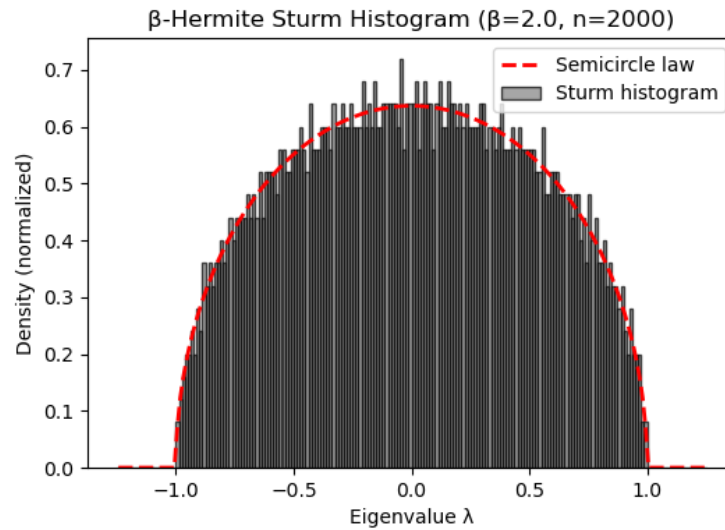


Figure 3: Sturm-based histogram for $\beta = 2$ reproduces the semicircle law for $n = 2000$.

1.3 β -Estimator via Wigner Surmise

1.3.1 Mathematical Background

While the exact nearest-neighbor spacing distribution for large- n ensembles is described by the Mehta and Gaudin (1960), it is computationally expensive to evaluate. In practice, the distribution is well-approximated by the Wigner Surmise (Wigner (1967)), which generalizes the exact spacing statistics of 2×2 matrices to the large- n limit. This approximation is given by:

$$P_\beta(s) = a_\beta s^\beta e^{-b_\beta s^2},$$

where the constants are:

$$b_\beta = \left(\frac{\Gamma\left(\frac{\beta+2}{2}\right)}{\Gamma\left(\frac{\beta+1}{2}\right)} \right)^2, \quad a_\beta = \frac{2 b_\beta^{(\beta+1)/2}}{\Gamma\left(\frac{\beta+1}{2}\right)}.$$

Therefore, given empirical spacings $s_i > 0$, we may estimate β by maximum likelihood:

$$\hat{\beta} = \arg \max_{\beta > 0} \sum_i \log(a_\beta) + \beta \log s_i - b_\beta s_i^2.$$

1.4 Combined Visualization Platform

I integrated the Sturm histogramming engine (Section 2) and β -estimator (Section 3) into a unified Gradio interface hosting on <https://huggingface.co/spaces/rosenyu/18338RMTProject>, providing:

- sliders for n , β , and number of histogram bins,
- real-time plotting of eigenvalue density using Sturm sequences,
- a text box for uploading spacing data and estimating β ,
- example data for testing,
- fully client-accessible source code.

The final application runs entirely on CPU and produces eigenvalue histograms of size $n = 2000$ in a fraction of a second, closely matching the performance predicted by the theory.

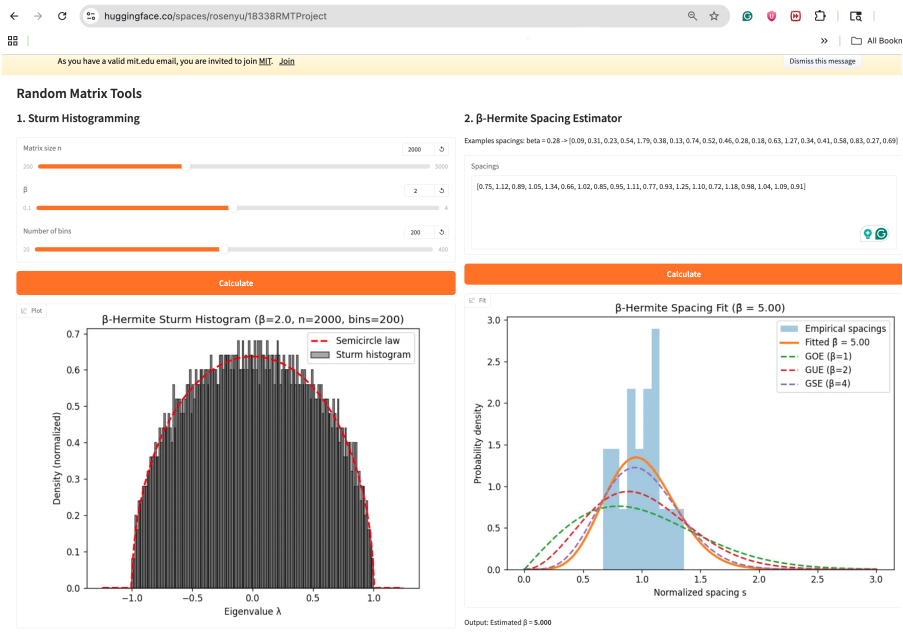


Figure 4: Gradio website UI for Sturm sequence histogramming and beta estimator.

2 Quantifying Repulsiveness in the β -Hermite Ensemble

2.1 Motivation

One open question in the β -Hermite ensemble research is: how can we quantify the spatial “repulsion”? As emphasized in Dumitriu and Edelman (2006)’s tridiagonal representation, increasing β strengthens short-range repulsion while reducing eigenvalue fluctuations. Recent work in determinantal point process (DPP), a general approximation using β -Hermite ensemble in the $\beta = 2$ case, came up with metrics measuring the repulsiveness. The general framework developed in Biscio and Lavancier (2016) identifies the pair-correlation function

$$g(r) = \frac{\rho^{(2)}(x, x + r)}{\rho^2}$$

as the central object for measuring repulsiveness in DPPs. Repulsiveness manifests as the departure of $g(r)$ below the Poisson baseline (the typical `rand()` sampler) $g(r) \equiv 1$. Biscio and Lavancier (2016) demonstrate that both local behavior (small-r expansion), global structure ($\int(1 - g)$), and nearest-neighbor distributions encode different aspects of repulsion. Thus, in this project, we will Biscio and Lavancier (2016)’s proposed metric to quantify the “repulsion” in β -Hermite ensemble.

Let $g_\beta(r)$ denote the numerically estimated pair-correlation function for the β -Hermite ensemble. Four quantitative measures of repulsion are used.

2.2 Metrics

2.2.1 Global Repulsion

Following Biscio and Lavancier (2016), global repulsiveness is measured by

$$R_{\text{global}} = \int_0^\infty (1 - g_\beta(r)) dr$$

This integral measures the total ”area” of the repulsion hole around a particle. A larger value implies stronger global inhibition between points.

2.2.2 Local Repulsiveness

Repulsiveness is also characterized locally by the behavior of points at very small distances. Biscio and Lavancier (2016) quantify local repulsiveness using the Laplacian of the pair correlation function at the origin, $\Delta g(0)$. In our 1D isotropic context, this corresponds to the curvature (second derivative) at zero:

$$\mathcal{R}_{\text{local}} = g_\beta''(0)$$

For β -Hermite ensembles, theoretical asymptotics suggest $g(r) \sim r^\beta$ Dumitriu and Edelman (2006) near zero. Consequently, we expect $g''(0)$ to capture the convexity of the repulsion hole, providing a metric highly sensitive to β .

2.2.3 Spacing Distribution Distance

While R_{global} captures global rigidity, the local fluctuation properties are classically described by the nearest-neighbor spacing distribution, $p(s)$, where s represents the distance between adjacent particles $s_i = x_{i+1} - x_i$. As β varies, the shape of $p(s)$ transitions from the exponential distribution of a Poisson process (e^{-s}) to the unimodal Wigner surmise distributions. We quantify the divergence from randomness by calculating the L_1 distance (Total Variation Distance) between the empirical spacing distribution $p_\beta(s)$ and the Poisson baseline:

$$\mathcal{D}_{\text{spacing}} = \int_0^\infty |p_\beta(s) - e^{-s}| ds$$

This metric provides a scalar value representing how distinct the short-range spacing statistics are from a non-interacting random process.

2.3 Numerical experiment of metrics calculation and Results

We performed numerical experiments on β -Hermite ensembles with matrix size $N = 500$ across a range of $\beta \in [0.1, 0.3, 0.5, 0.8, 1, 2, 3, 4, 5, 6, 7, 8, 9, 10]$. For each β , we generated 300 trials to estimate the pair correlation function $g_{\beta}(r)$ and the nearest-neighbor spacing distribution $p(s)$, and calculate the three metrics proposed. We also compute the metric on a baseline random sampler `rand()` as our “Poisson baseline”. The results

illuminate three distinct aspects of repulsion: spectral rigidity, local hard-core exclusion, and lattice regularity. We plot the mean and standard deviation (with standard deviation shown as the hue) across trials in our result plots.

2.3.1 Saturation of Global Repulsiveness

Figure 5 illustrates the Global Repulsion metric, $\int(1 - g(r)) dr$, which acts as a proxy for the “Probability of Difference” p_u proposed by Møller and O’Reilly (2021). It is shown that the metric rises sharply from the Poisson baseline ($\beta \rightarrow 0$) and quickly saturates at a constant value for $\beta \gtrsim 1$.

This saturation confirms the Sum Rule inherent to Coulomb gas systems. Unlike Poisson processes, where density fluctuations scale with the square root of the volume, β -Hermite ensembles are **hyperuniform** (or rigid). The presence of a particle at a specific location necessitates a total deficit of exactly one particle in the surrounding space to conserve the global number of eigenvalues. This metric successfully distinguishes a random matrix system from a Poisson system, but as predicted by theory, it does not differentiate between different non-zero values of β , as the total integrated deficit is conserved regardless of the interaction strength.

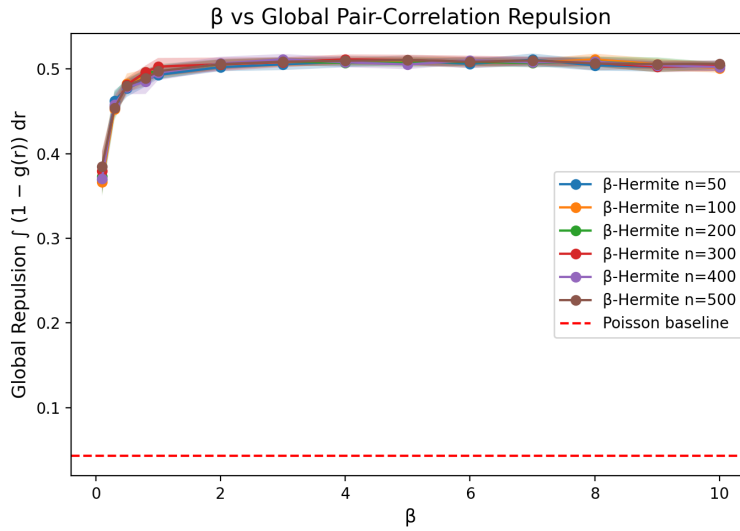


Figure 5: Global repulsion index $\int(1 - g_\beta) dr$ increases gradually with β , capturing long-range depletion relative to Poisson.

2.3.2 Non-Monotonicity of Local Repulsiveness

Figure 6 displays the curvature of the pair correlation function at the origin, $g''(0)$, derived from the metric proposed by Biscio and Lavancier (2016). It is shown The metric is non-monotonic, peaking around $\beta \approx 3$ and decreasing toward zero for large β . This trend captures the changing shape of the repulsion hole. Theoretical asymptotics state that $g(r) \sim r^\beta$ near the origin.

- For small β (e.g., $\beta = 1$), the hole is V-shaped (linear), resulting in moderate curvature.
- As β increases to ≈ 3 , the hole widens into a U-shape, maximizing the second derivative.
- For large β (e.g., $\beta = 10$), the repulsion becomes “hard-core,” and the function r^β becomes extremely flat at the origin (a “flat-bottomed” basin). Mathematically, the second derivative of r^{10} at zero is 0. Thus, the decrease at high β indicates *stronger* repulsion (a wider forbidden zone), not weaker.

Monotonic Increase in Spacing Regularity Figure 7 (Spacing Distance) and Figure 8 (Scatter Plots) capture the “crystallization” of the eigenvalues. The Spacing Distribution Distance ($\mathcal{D}_{\text{spacing}}$) increases monotonically with β , approaching an asymptote.

This metric is the most effective for distinguishing between different degrees of repulsion. As β increases, the system transitions from a “gas” state (irregular spacing, Figure 8 top-left) to a “crystal” state (quasi-lattice, Figure 8 bottom-right). The spacing distribution $p(s)$ transforms from an exponential curve (Poisson) to a Gaussian-like peak centered at 1. The $\mathcal{D}_{\text{spacing}}$ metric quantifies the Total Variation distance of this transition, showing that the arrangement of eigenvalues becomes deterministically regular as the inverse temperature β increases.

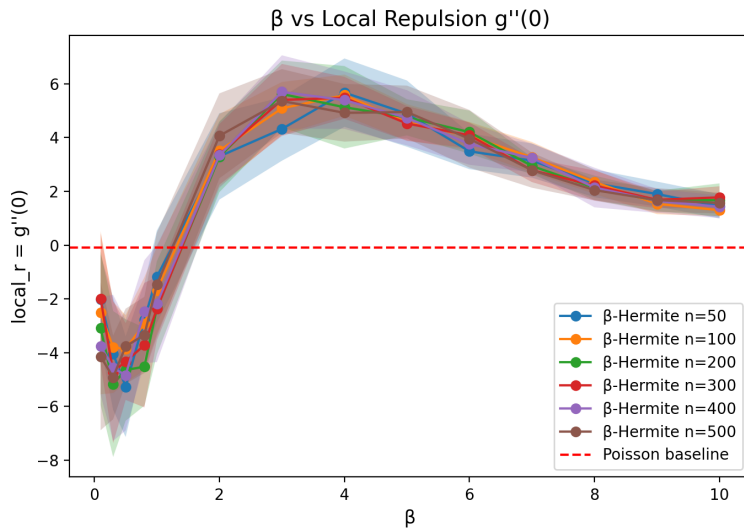


Figure 6: Local repulsion curvature $g''_\beta(0)$ peaks at intermediate β , consistent with the small- r expansion $g_\beta(r) \sim r^\beta$.

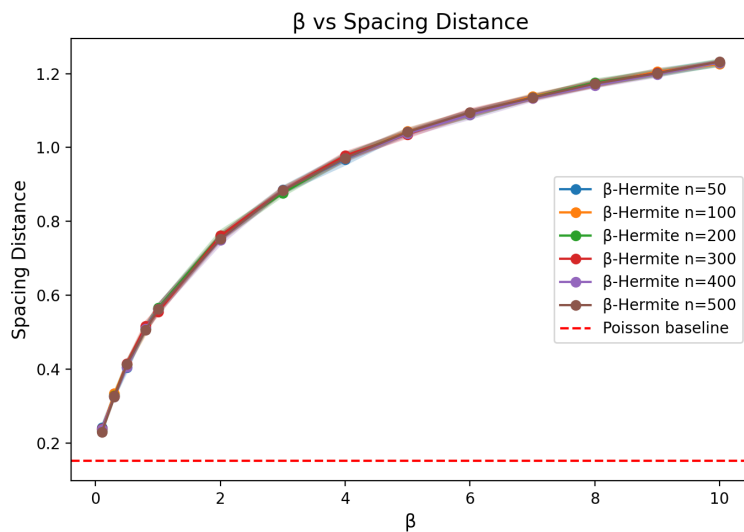


Figure 7: Nearest-neighbor repulsion index R_{nn} decreases sharply for small β and saturates as the spacing distribution becomes strongly non-Poisson.

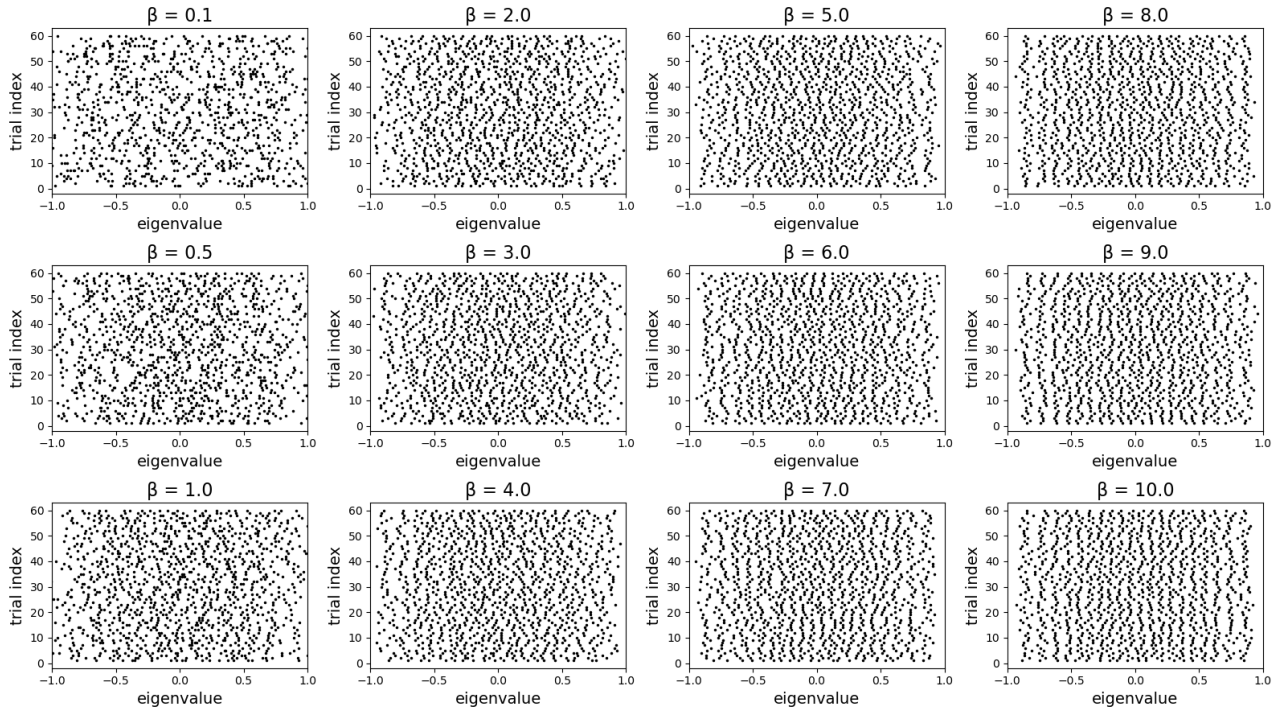


Figure 8: Eigenvalue scatter plots across β illustrate the qualitative transition from irregular spacing (small β) to quasi-lattice behavior (large β).

References

- Albrecht, J. T., Chan, C. P., and Edelman, A. (2009). Sturm sequences and random eigenvalue distributions. *Foundations of Computational Mathematics*, 9(4):461–483.
- Biscio, C. A. N. and Lavancier, F. (2016). Quantifying repulsiveness of determinantal point processes.
- Chan, C. P. (2007). *Sturm sequences and the eigenvalue distribution of the beta-Hermite random matrix ensemble*. PhD thesis, Massachusetts Institute of Technology.
- Dumitriu, I. and Edelman, A. (2006). Global spectrum fluctuations for the β -hermite and β -laguerre ensembles via matrix models. *Journal of Mathematical Physics*, 47(6).
- Mehta, M. L. and Gaudin, M. (1960). On the density of eigenvalues of a random matrix. *Nuclear Physics*, 18:420–427.
- Møller, J. and O'Reilly, E. (2021). Couplings for determinantal point processes and their reduced palm distributions with a view to quantifying repulsiveness. *Journal of Applied Probability*, 58(2):469–483.
- Trefethen, L. N. and Bau, D. (2022). *Numerical linear algebra*. SIAM.
- Wigner, E. P. (1967). Random matrices in physics. *SIAM review*, 9(1):1–23.
- Wilkinson, J. H. (1988). *The algebraic eigenvalue problem*. Oxford University Press, Inc.